

Data-driven machine learning model to predict the effective
coupled properties of magneto-electro-elastic auxetic
structures

Mohamed Amine Bakkoury

Supervised by Prof. Vinyas Mahesh & Prof. Sathiskumar A Ponnusami

Abstract

This project explores the prediction of auxetic natural frequencies in structures using machine learning (ML) models. The dataset consists of descriptive features related to material and geometry, along with natural frequencies. Through data analysis and ML model implementation, relationships between traditional and auxetic frequencies are examined.

Moreover, the project discusses the possibility of applying the modeling approach to study magneto-electroelastic (MEE) materials, enabling predictions of their coupled properties. This integration of ML and finite element analysis could provide valuable insights and potentially replace traditional analysis methods.

Overall, this research demonstrates the effectiveness of ML models in predicting auxetic natural frequencies and their potential for advancing knowledge in the field of auxetic structures. The findings contribute to the understanding of material properties, geometry, and their impact on auxetic eigenfrequencies, paving the way for future applications in various domains.

Contents

Introduction	4
1 Context on Magneto-Electro-Elastic materials	6
2 Motivations and objective	6
3 Design	7
4 Machine learning for modeling behavior of auxetic structures	8
5 Data collection and problem formulation	9
5.1 COMSOL Simulations	9
5.2 Problem formulation	12
6 Data analysis and modeling implementation	12
6.1 Exploratory data analysis	12
6.2 Data preparation	15
6.3 Model selection	16
7 Results interpretation	17
7.1 Model performance	17
7.2 Error analysis	17
7.3 Feature importance	18
8 Applications and limits	20
9 Discussion	21
Appendix	24
A Exploratory data analysis	24
B Error Analyis	26
C MATLAB script for COMSOL simulations automation	26

Introduction

Due to their advantageous mechanical properties and potentially transformative applications in various sectors, auxetic structures have garnered significant attention and research from many industries. Unlike conventional materials, which tend to contract, or remain unchanged under tensile forces, auxetic structures will expand in the lateral direction, and inversely, will contract instead of expanding under a compressive load.[17] This unusual feature is expressed through the structure's Poisson's ratio, which is a non-dimensional property that describes the ratio of a lateral strain (expansion or contraction) to a longitudinal strain (tensile or compressive) when subjected to an external load.

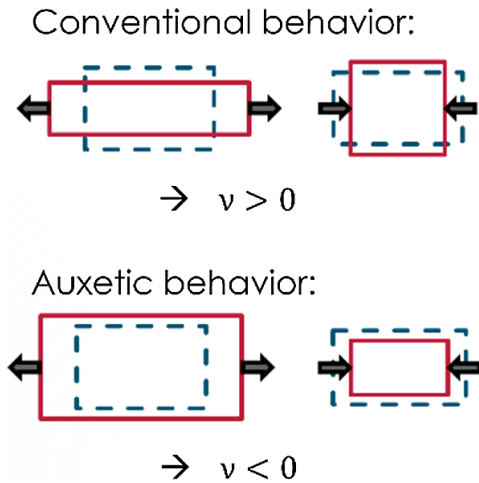


Figure 1: Behavior difference between conventional and auxetic materials[21]

Values for Poisson's ratio usually lay in the 0 to 0.5 range. Structures or materials with a negative Poisson's ratio, however, are known as auxetic. This property has been studied since as early as the 1980's, with the term being coined by Professor Ken Evans of the University of Exeter in 1991, who even predicted the accelerating interest and ever increasing applications of auxetics, stating "Some of these applications will be reached in the near future, others will require many years of development. The main point to make is that auxetic materials are not just a curiosity, they are also very useful.". (Evans, 1991) [3][1].

In line with Professor Evans' prediction, auxetics have shown excellent properties in a variety of applications. One such property is their increased resistance to shear stress caused by twisting or tearing forces. This can be understood mathematically through the relation Poisson's ratio has with shear, Young's and bulk modulus. Additionally, auxetics do not dent as much as traditional materials. Thanks to their shape, when subjected to an impact, an auxetic material will compress towards the point of impact, thus increasing its local density and making it more resistant to indentation. Auxetics have also proven useful in damping and acoustic absorption applications, where auxetic foams have been observed to exhibit better absorption capacities than conventional foams at all frequency levels.[6][9] Because of these exceptional properties, amongst others, auxetics have found themselves used in a myriad of applications, from sports and textile engineering, to defence and aerospace.[6][14]

Considering all the benefits and potential applications of auxetics, it is no surprise that they have been attracting more academic attention over the past few years. In fact researchers have explored various approaches, including analytical models, numerical simulations, and experimental investigations, to study and characterise auxeticity in different materials and geometries. These studies have shed light on the complex relationship between the internal architecture of auxetic structures and their mechanical response. [10][13][15] As exemplified by these studies and many more in this field, with recent advancements in computational modelling, there has been a shift toward

employing sophisticated techniques such as finite element analysis, computational optimization, and machine learning to enhance our understanding and design capabilities of auxetic structures. These computational methods enable researchers to simulate and predict the behaviour of auxetics under different loading conditions, analyse the effects of various parameters, and optimise the structures for specific applications.[19][20]

There has also been a significantly growing interest in using composite materials that can incorporate piezoelectric and piezomagnetic phases in the development of smart structures. This interest can be attributed to their ability to convert magnetic, electric and mechanical energies into one another, allowing for interactive transformation between each of these energy types.[2] One example of such composites are magneto-electro-elastic materials (MEEs). They represent a unique category of smart materials, given their layered structure, which allows them to benefit from unique piezoelectric and piezomagnetic phases. As such, they demonstrate excellent interaction between their electric, magnetic and elastic fields, making them highly valuable in a variety of applications.[8]

As with auxetics, this ever increasing attention into MEEs has translated into an increase of studies, analyses and reviews into their behaviour. One specific area of interest is the MEE's vibrational responses, which can be assessed through their natural frequency. Studying the natural frequency of magneto-electro-elastic materials provides valuable insights into their vibrational behaviour, allowing us to understand and optimise their performance in applications related to energy harvesting, sensing, and structural health monitoring.[4] Natural frequency studies also grant information regarding a structure's modal shapes, which can provide valuable insights for assessing structural integrity, optimising designs, controlling noise and vibrations. In the case of MEEs, research conducted on them has shown that their natural frequencies were influenced by the coupling between their different fields, as well as the geometrical characteristic of the structure studied. Furthermore, the structure's boundary conditions were also shown to have a significant effect on the natural frequency of the studied MEE structures.**[mees_model_2][11]**

Most of the aforementioned studies were conducted with the aid of powerful computational methods, such as finite element analysis (FEA) which is widely used in engineering and design. One of the significant benefits of FEA is its ability to provide detailed insights into complex structural behaviour. This enables engineers to analyse stress distribution, deformation, and other critical parameters, helping in design optimization, identifying potential weak points, and ensuring structural safety. It also allows for virtual prototyping, saving time and cost associated with physical testing. Engineers can iteratively refine designs, exploring different configurations, materials, and boundary conditions virtually. This facilitates faster product development cycles, reduced reliance on physical prototypes, and enables efficient optimization. [25][16] However FEA does come with its limitations. Firstly, the accuracy of FEA results heavily relies on the assumptions made during model development. Simplifications in geometry, material properties, and boundary conditions can introduce errors and affect the reliability of predictions. Another limitation is the computational cost and time required for complex analyses. FEA involves solving large systems of equations, which can be time-consuming and computationally intensive. This can limit the scale and complexity of problems that can be solved within a reasonable timeframe. [7][23]

This report aims to explore the impact of auxeticity on MEE materials by predicting their behaviour in terms of natural frequencies using a data-driven machine learning (ML) model. The process begins with designing the relevant auxetic structures utilising computer-aided design (CAD) software, specifically SolidWorks. These designed structures are then imported into COMSOL Multiphysics®, where eigenfrequency analysis is conducted to gather essential data. The collected data from the COMSOL analysis serves as the training dataset for the ML model. Finally, the report evaluates potential applications based on the insights gained from the information collected throughout this study.

1 Context on Magneto-Electro-Elastic materials

As mentioned briefly in the introduction, Magneto-Electro-Elastic (MEE) materials are a special kind of composite smart materials that can demonstrate both magnetostrictive and piezoelectric properties simultaneously. This essentially means that they are capable of converting mechanical energy into its electrical form, and the other way around, while additionally having the capacity of converting mechanical energy into magnetic fields and again, the other way around. This unique set of properties allows them to be relevant in a wide range of applications, across different industries. [5]

Magnetostriction refers to the ability certain materials have to experience mechanical strain when subjected to a magnetic field. This occurs due to these material's internal structures which is essentially divided into different disorganised domains of identical magnetic polarisation. When an external magnetic field is applied, these domains all rearrange according to the field's direction, resulting in internal mechanical strain. The inverse of this is also true, with magnetostrictive materials experiencing changes in their magnetic state under the influence of an external load. [18]

Piezoelectricity, on the other hand, describes the ability certain materials have to generate an electric charge when subjected to an external load. This occurs thanks to an asymmetry in these materials' internal crystal structure, leading to the displacement of positive and negative, which results in the generation of an electric charge.[24]

In MEEs ,the coupling between magnetostriction and piezoelectricity occurs due to the interaction between their respective magnetic and electric fields. More precisely, when both fields are present, they interact with the material's crystal structure, leading to the aforementioned coupling effect. This effect allows for the manipulation of MEE's mechanical response by subjecting them to electric and magnetic fields.

MEE materials find extensive applications in the development of actuators and sensors. The ability to convert electrical and magnetic energy into mechanical strain allows for precise control and manipulation of these devices. They are employed in systems requiring high precision, such as micropositioning devices, adaptive optics, and ultrasonic transducers.[22]

MEE materials can be utilised for energy harvesting applications, where mechanical vibrations or environmental vibrations are converted into electrical energy. These materials can efficiently capture energy from various sources, such as machinery vibrations, ocean waves, and ambient vibrations, making them promising candidates for self-powered systems and wireless sensor networks.

Their properties enable the development of adaptive structures that can change their mechanical properties in response to external stimuli, as such they are used to design vibration control systems that actively attenuate vibrations and noise. This, in turn, allows them to find applications in a wide variety of fields where vibration control and structural integrity are primordial.

2 Motivations and objective

The primary objectives of this study are centred around the design and implementation of a machine learning (ML) model with the ability to predict the effect of auxeticity on various honeycomb structures. While the traditional approach involves simulating these structures directly using computer-aided design (CAD) software, this method often proves computationally expensive. Therefore, the overarching goal of this research is to explore an alternative path that eliminates the dependence on such software beyond the initial design phase.

Investigation of the natural frequency of these structures holds significant importance. It plays a crucial role in ensuring the safe design of honeycomb structures by addressing several key factors. Firstly, understanding the natural frequency helps in avoiding resonance phenomena, which

can lead to catastrophic failures or excessive vibrations. By predicting and controlling resonance, structural integrity and performance can be significantly enhanced.

Controlling vibrations is yet another advantage that can be gained from studying the natural frequency of honeycomb structures. By manipulating the frequency response and mode shapes, it becomes possible to minimise undesirable vibrations or disturbances, particularly in applications where vibration control is crucial, such as aerospace or automotive engineering.

In summary, this study aims to develop an ML model for predicting the effect of auxeticity on honeycomb structures, offering a cost and time effective alternative to traditional simulation methods. By analysing the natural frequencies of these structures, crucial insights can be obtained, enabling safe design practices. The outcomes of this research have the potential to advance structural design practices and unlock the benefits of auxetic structures in a wide range of industries and applications.

3 Design

The design steps for this study started on Abaqus, a computer-aided engineering (CAE) and FEA software, on which the geometric structures to be studied were be designed. First, individual cells that form the honeycomb structures were sketched, before being arranged at an appropriate distance to create a 1mm gap, which will represent the thickness of the structure. The linear sketch pattern tool was then utilised to generate the honeycomb pattern. This pattern was then extruded to create a three-dimensional shape, which served as the core for the final structures. To complete the structures, top and bottom layers were created using the geometry of the respective cores. These layers were designed as plates that would encapsulate the core and provide structural integrity.

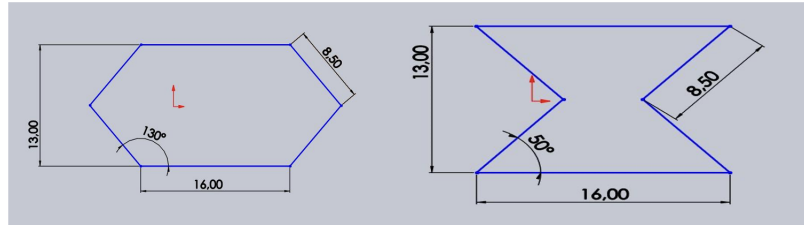


Figure 2: Example of a hexagonal unit cell (left) and the matching auxetic unit cell (right)

	Auxetic Re-entrant				Hexagonal Honeycomb			
Geometry #	1	2	3	4	1	2	3	4
Dimensions*								
Cell Angle, θ	30	50	70	60	150	130	110	120
Unit Cell Height, h	6.92	13.00	27.50	34.64	6.92	13.00	27.50	34.64
Base Length, l_1	20	16.00	25.00	30.00	20	16.00	25.00	30.00
Side Length, l_2	6.92	8.50	14.60	20.00	6.92	8.50	14.60	20.00
Structure Height, H	31.68	56	114.00	161.52	39.60	72	143.45	178.20
Structure Length, L	127.00	92.93	154.96	142.56	197.00	162.80	220.56	292.84

Figure 3: Structure and unit cell geometries (Distances are in mm and angles in degrees)

The cores and plates were assembled to form the complete structures, ready for simulation. Before proceeding with the simulation and frequency analysis, the auxeticity of the structures was tested. This was accomplished by subjecting the structures to a tensile force applied normally to the top layer and clamping the bottom layer.

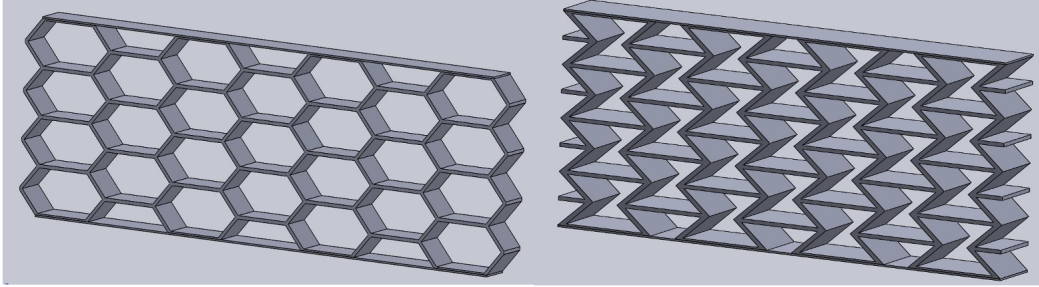


Figure 4: Completed structures for hexagonal and auxetic geometries #1

During testing, it was expected that the auxetic re-entrant honeycomb cores would expand under the tensile force, while the traditional hexagonal cores would contract.

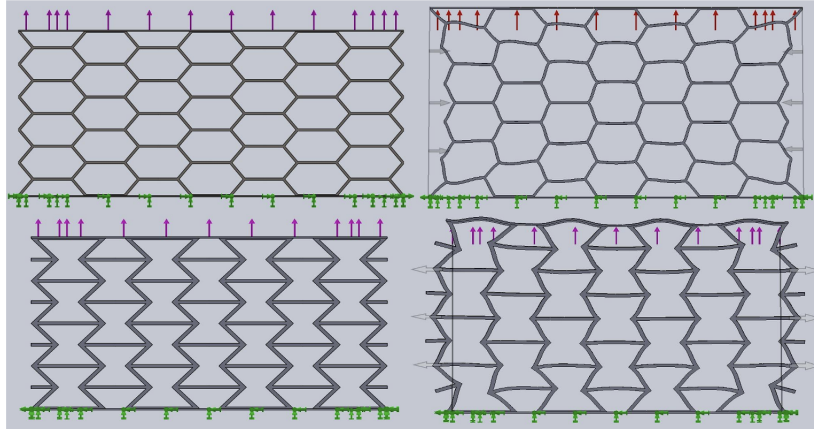


Figure 5: Testing auxeticity of the finalised structures

As can be observed in Fig 5, each structure exhibited the response that was expected given their design, confirming the auxeticity of the structure at the bottom. This test was performed on the remaining structures, which all had this same response.

With the design steps completed and confirmed to behave the way they are expected to, the foundation has been set for the subsequent simulation and frequency analysis of the structures.

4 Machine learning for modeling behavior of auxetic structures

This project aims at exploring the modeling of auxetic materials using machine learning (ML) methods. The property on focus here is the natural frequencies of these materials. In particular, given a material, its geometry, and knowing its hexagonal natural frequencies, we would like to understand how accurately can an ML model be at predicting its auxetic natural frequencies. Given the exploratory nature of this work, public dataset that we could use to train such models is very limited. Therefore, we leveraged a finite element analysis (FEA) software (namely COMSOL) to build a dataset. In this context, one could wonder why building an ML model that predicts a property that can be simulated. This is a central question, that can have several answers:

- ML models are faster

ML models offer significant advantages when compared to traditional FEA analysis in predicting the behavior of auxetic structures. Firstly, ML models are faster in terms of both training and prediction time. FEA analysis typically involves complex numerical computations that can be time-consuming and computationally expensive, especially for large and intricate structures. In contrast, ML models can quickly learn patterns and make predictions based on the input data, significantly reducing the computational time required.

- Ease of use

Secondly, ML models tend to be more user-friendly. FEA analysis often requires expertise in numerical methods and many engineering principles, making it less accessible to non-experts. ML models, on the other hand, can be trained using large datasets and automated algorithms, making them more user-friendly. This accessibility enables a broader range of users, including designers and engineers with limited programming knowledge, to leverage ML for auxetic structure prediction.

- Sensitivity analysis and optimization

ML models also facilitate sensitivity analysis and optimization of auxetic structures and beyond. By training ML models on various input parameters and analyzing their impact on the predicted behavior, it becomes possible to identify key influential factors and optimize the design accordingly. This capability enhances the understanding of how different variables affect auxetic behavior and enables engineers to refine their designs more efficiently.

- Extrapolation and interpolations

Another advantage of ML models is their ability to perform extrapolation and interpolations. Traditional FEA analysis often relies on discretized meshes and limited input data, which can be limiting when it comes to the accuracy of predictions beyond the trained range. ML models, however, are able to generalize from learned patterns and make predictions for input combinations that lie outside the training data. This extrapolation capability allows for more comprehensive exploration and provides valuable insights into the behavior of auxetic structures in unexplored regions.

- Scalability

Scalability is another strength of ML models. FEA analysis can be computationally demanding, particularly when dealing with large-scale or multi-scale systems. ML models can be trained on high-performance computing platforms and parallelized to handle large datasets and complex structures efficiently. This scalability enables the analysis of larger and more intricate auxetic structures, expanding the scope of applications for predictive modeling.

- Integration with other systems

Lastly, ML models can be integrated with other systems seamlessly. They can be embedded within existing design software, as has been done in this study, or integrated into automated design optimization processes. This integration allows for a synergistic approach where ML models enhance the analysis and decision-making capabilities of existing engineering tools. By exploiting the strengths of ML and traditional engineering methods, designers and engineers can benefit from a more comprehensive and efficient design process for auxetic structures and potentially apply it to other fields.

5 Data collection and problem formulation

5.1 COMSOL Simulations

The first step was to import the SolidWorks model files into COMSOL Multiphysics, the software used for the simulations. This allowed for the models to be accurately represented in the simulation environment. Once the model was imported, the setup for eigenfrequency computation was performed. This involved several key tasks:

- Importing the solid mechanics physics onto the model: This step ensured that the appropriate physics behaviour was applied to the structure for the eigenfrequency analysis.
- Setting up the correct boundary conditions: The boundary conditions were defined to represent the desired constraints or constraints-free nature of the structure. This step played a crucial role in accurately capturing the structural behaviour.
- Attributing a material to the model: Assigning the appropriate material properties to the model was essential for capturing the material behaviour accurately during the simulations.
- Building a mesh for the model: A mesh was created to discretize the model into smaller elements, enabling efficient computation and accurate representation of the structure's geometry. A convergence test was done around the fundamental frequency of one of the structures to determine the mesh size used for the rest of this paper.

Mesh Size	Fundamental Freq.	Time to solve (s)	DoFs solved
Normal	2121 Hz	12	181,908
Fine	2092.3 Hz	23	365,925
Finer	2085.7 Hz	45	751,278
Extra Fine	2079.8 Hz	80	1,191,414

Figure 6: Convergence tests

- Though the Finer and Extra Fine meshes showed a slight increase in accuracy over the Fine one, the increased time and computational costs, illustrated by the time to solve and degrees of freedom solved, could not justify going for a mesh any finer than the Fine setting, especially considering the amount of times the eigenfrequency study will be ran throughout this paper.
- Creating the eigenfrequency study and setting up the necessary parameters: The eigenfrequency study was defined to perform the analysis and compute the eigenfrequencies of the structure. The relevant parameters, such as the desired frequency range and precision settings, were appropriately set up for the study.

Once the simulations were executed, the eigenfrequencies and corresponding modal shapes associated with each frequency were obtained. These results provided valuable insights into the dynamic behaviour of the structures, which were crucial for further analysis. To train the machine learning (ML) model successfully and predict the effect of auxeticity on the structures, sufficient data points needed to be collected. This required tweaking different parameters to gather a wide variety of data points and optimise the ML model's performance.

The first parameter to consider was the geometry of the structures. Four pairs of structures were designed, consisting of an auxetic honeycomb and a traditional hexagonal honeycomb. These different geometries allowed for a comprehensive exploration of the impact of auxeticity on the structures. Next, the boundary conditions were varied. The structures had two boundaries, the top and bottom layers, which offered three different setups for running the simulations: both clamped, one fixed, and both free. This allowed for analysing the influence of different boundary conditions on the structure.

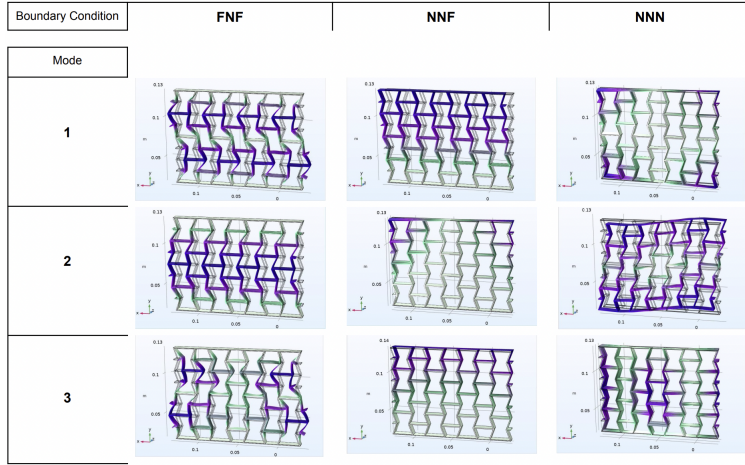


Figure 7: The effect of different boundary conditions on the first three modal shapes of one scenario tested

Finally, the material attributed to the model was considered. It was important to expose the ML model to data from a wide variety of materials to ensure its accuracy and relevance across different material properties.

Initially, the procedure for generating the data involved manually changing the parameters for each iteration and exporting the 10 eigenfrequencies after each iteration. However, this manual approach proved to be time-consuming and tedious, especially when considering large scale data collection. To overcome this challenge, the process was automated by exploiting the LiveLink feature of COMSOL. This feature allows the interaction with and execution of the model as a MATLAB script rather than a 3D structure within the COMSOL user interface by establishing communication between the two software tools through a COMSOL server.

Setting up any one of the study scenarios and exporting it as a MATLAB script essentially yielded a template that could be used to set up all the needed scenarios with a few tweaks to the base script. The script was analysed to identify the lines responsible for the parameters that needed to be changed for each iteration, which includes the model to be loaded, the material properties required for the simulation, and the boundary conditions. Given this information, it was now possible to automate the data collection process with minimal user intervention. This was achieved by creating a nested loop that iterates through each model, one at a time. Within each iteration, the eigenfrequency study was executed, under each of the three different boundary condition setups described. The first ten eigenfrequencies obtained from each scenario were then exported and saved into a text file.

The only remaining step requiring user intervention was providing the values for the three material properties - namely, Density, Poisson's ratio, and Young's Modulus - needed for each scenario. By inputting these values into the script, it became capable of generating and exporting the desired data for each studied scenario.

This automated approach enabled the generation of a larger dataset within a significantly shorter timeframe, avoiding the manual effort and potential for errors associated with changing parameters and exporting data individually.

The resulting dataset ended up spanning 2,520 rows by 13 columns. The first four columns describe which geometry was being tested through the different dimensions that define the different geometries. The next four describe the material used, with the name and each relevant material property being listed (Though the name was not used for anything other than data organisation). Finally, there is a column to define the boundary conditions and one to indicate which order

natural frequency is represented. The last two columns contained the matching eigenfrequency results which were computed from COMSOL.

5.2 Problem formulation

Let θ be the Machine learning model we are trying to build, X a set of descriptive features of the material and geometry, f_n^h the n^{th} order hexagonal natural frequency and f_n^a the n^{th} order auxetic natural frequency. The prediction task we want to perform is the following:

$$\hat{f}_n^a = \theta(X, f_n^h), \forall n \in [1, 10]$$

In other words, the objective is to build a regression model that predicts the auxetic natural frequencies based on descriptive data of the material and its geometry and the hexagonal natural frequency. (Note that, by design choice, we perform predictions on the 10 first natural frequencies. This ensures we have an important number of orders to study differences in modeling of these frequencies, while limiting the computation for data collection with COMSOL)

We have designed our dataset in order to be able to build a supervised learning model. In this paradigm, the model is provided with a set of input-output pairs (training examples) to learn the relationships (or patterns) between the input variables (explanatory variables) and the target variable that we try to predict. This is the reason we have simulated auxetic natural frequencies on COMSOL.

6 Data analysis and modeling implementation

6.1 Exploratory data analysis

Material physical properties

First of all, to better understand the collected data and what challenges we may face during the modeling phase, we performed an exploratory data analysis of the COMSOL simulations' outputs. Below is a sample of the collected dataset (the 12 first columns being the explanatory variables and the last one the target variable)

	unit_cell_height	base_length	side_length	structure_height	structure_length	material	young_modulus	density	poisson_ratio	boundary_conditions	frequency_order	hexagonal_eigenfrequency	auxetic_eigenfrequency
0	13.0	16.0	8.5	72.0	162.8	Steel	2.05000e+11	7850	0.28	FNF	1	2092.3	1691.1
1	13.0	16.0	8.5	72.0	162.8	Steel	2.05000e+11	7850	0.28	FNF	2	2833.1	3736.0
2	13.0	16.0	8.5	72.0	162.8	Steel	2.05000e+11	7850	0.28	FNF	3	2850.0	3858.7
3	13.0	16.0	8.5	72.0	162.8	Steel	2.05000e+11	7850	0.28	FNF	4	3667.2	4067.8
4	13.0	16.0	8.5	72.0	162.8	Steel	2.05000e+11	7850	0.28	FNF	5	3783.0	4447.3

Figure 8: Dataset sample

First, we visualized the different materials collected along with their physical properties. The charts below display each material and its Poisson ratio, Young modulus and density

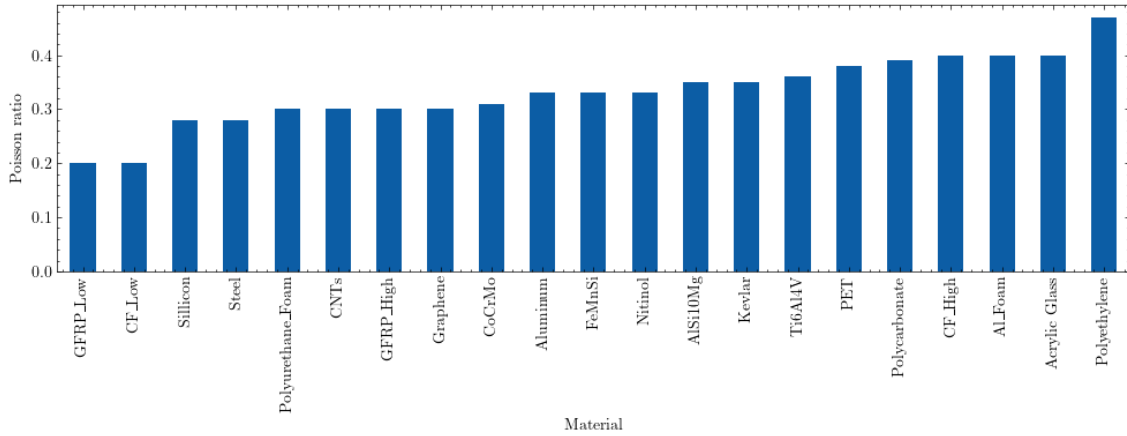


Figure 9: Materials modeled and their Poisson ratio

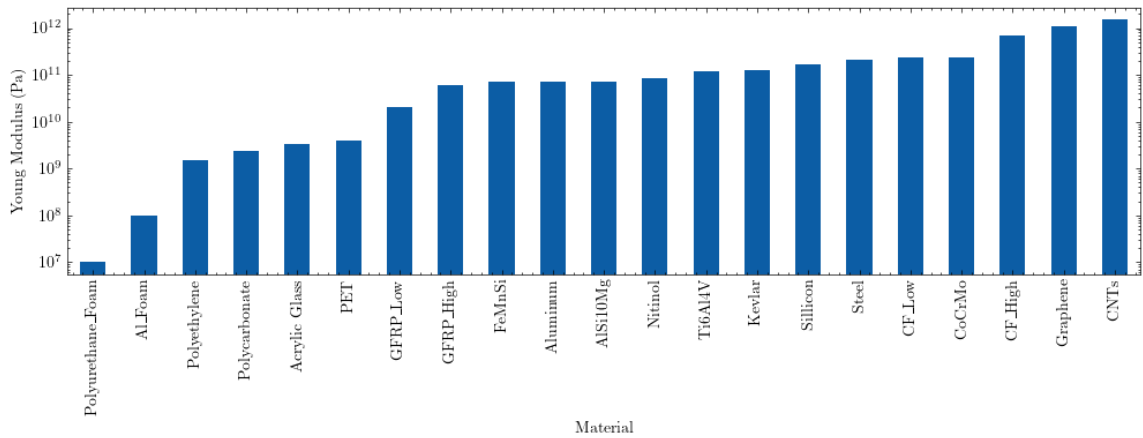


Figure 10: Materials modeled and their Young modulus (in Pa) - log scale

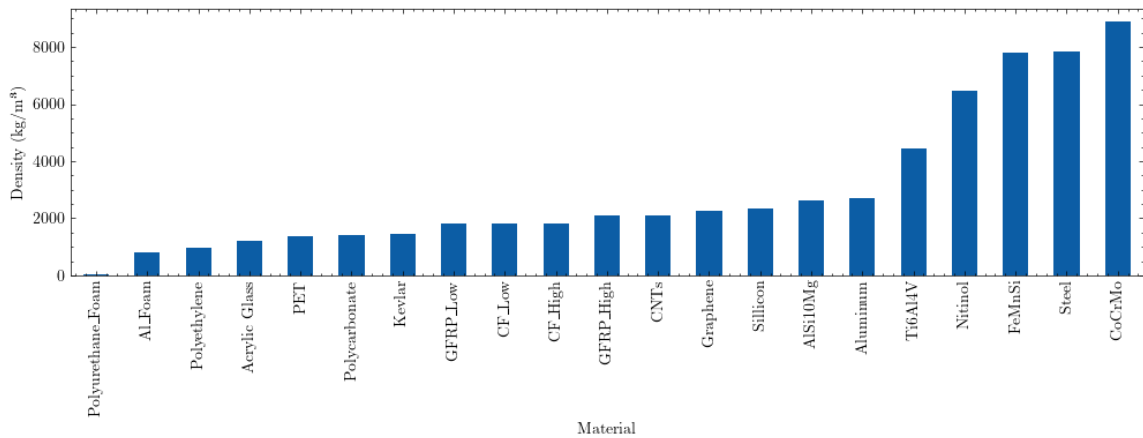


Figure 11: Materials modeled and their density (in kg/m^3)

We designed the data collection step to ensure we have a satisfying diversity of materials in our dataset (in terms of physical properties), and be able to study their impact on the auxetic structure's eigenfrequencies. In section 7, we propose an estimation of these parameters' influence on the auxetic eigenfrequencies.

Hexagonal eigenfrequency

Intuitively, we can expect hexagonal and auxetic eigenfrequencies to be highly correlated. Indeed, these are natural frequencies of the same material under different shapes. This intuition can be verified by running an analysis of the relation between hexagonal and auxetic eigenfrequencies variables. First, we ran the following unidimensional regression:

```
auxetic_eigenfrequency ~ hexagonal_eigenfrequency
```

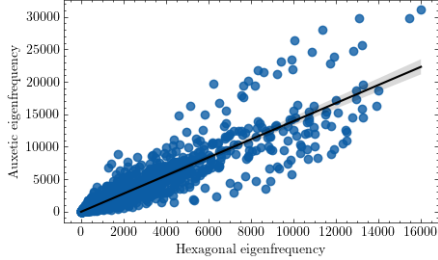


Figure 12: Regression plot for $f^a \sim f^h$

The relationship between variables is statistically significant according to this analysis ($p = 0.00$, see A for regression table), with an R^2 of 0.83. In other words, the hexagonal eigenfrequency accounts for 83% of the variability of the auxetic frequency. This confirms our intuition and indicates that the hexagonal eigenfrequency will be a crucial feature when building our ML model.

In order to better understand this relation, we further analyzed the correlation between the two structures' natural frequencies, but this time breaking down by frequency order. Our objective being to understand if all order frequencies are similarly correlated. We have conducted 10 unidimensional linear regressions for each of the frequency orders ($f_n^a \sim f_n^h, \forall n \in [1, 10]$). The results are shown in the charts below:

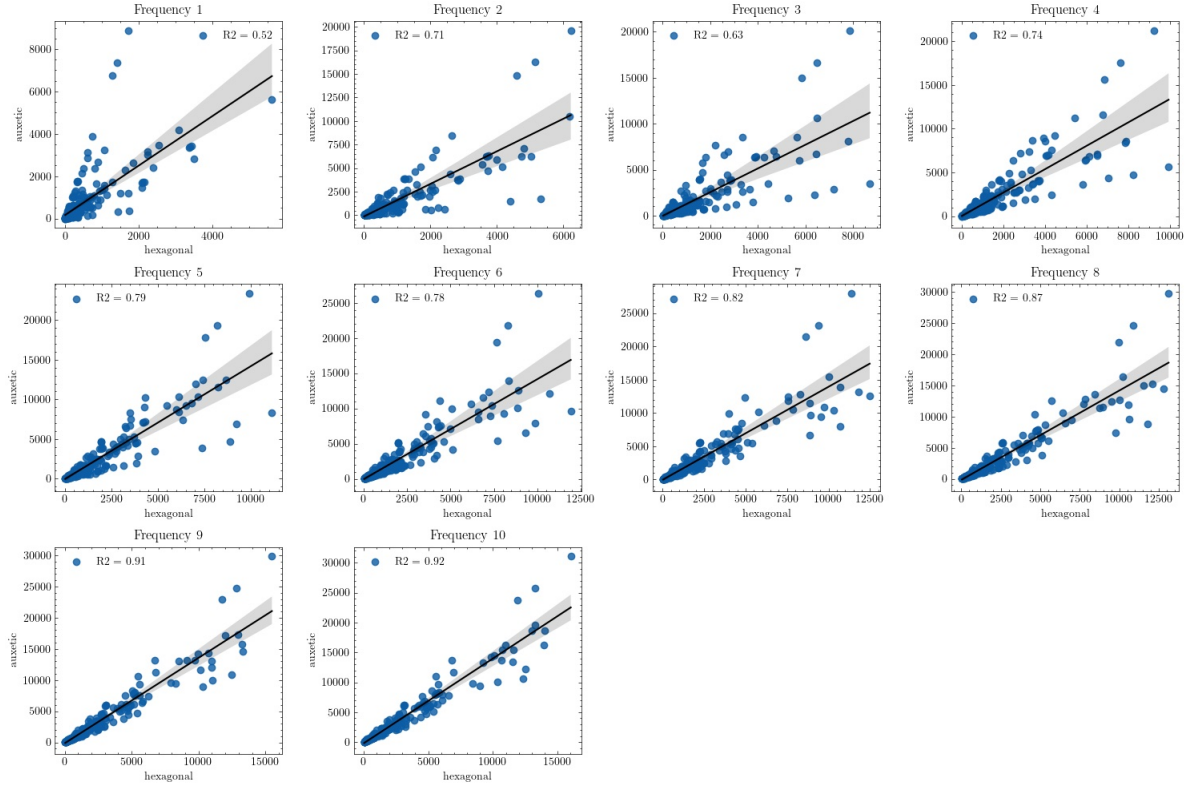


Figure 13: Individual unidimensional linear regressions for each eigenfrequency order

This analysis reveals heterogeneous relationships between the variables depending on the order of the frequency. In particular, the correlation is much lower for f_1 ($R^2 = 0.52$) than f_{10} ($R^2 = 0.92$). Indeed, we observe many outliers in the first scatterplot, revealing that the auxetic frequency is often much higher than the hexagonal one (this is aligned with histograms of both variables, referenced in A, figure 20). This indicates that we will face challenges building a model that generalizes well to all eigenfrequencies.

6.2 Data preparation

The first step of our modeling process is to prepare data to be ingested by an ML model. Before doing that, we split our dataset into a training and a test set. This step is crucial as it will allow us to evaluate the model we will build on data that hasn't been exposed to during the training process. Indeed, we want our model to be robust to new materials and geometries and adapt well to predict unseen frequencies. To perform this split, we make sure no material is both in the training and the test set (the splitting is done based on the materials). Our dataset is composed of 23 materials, that we divide as follows:

- 3 materials compose the **test set**: namely *Silicon*, *CoCrMo* and *Graphene* (Sample size of 360)
- The remaining 20 materials compose the **training set** (Sample size of 2000)

Moving forward, the model will be trained on the training set and evaluated on the test set.

Before starting to build and compare different models on our data, it needs to be processed to be in a suitable format to be processed by an algorithm. Following is an overview of the manipulations performed:

- Convert columns to the appropriate data type: e.g.: Young modulus was a string in the original dataset and is converted to a float)

- Normalize numerical variables (to make sure all features are on comparable scales)
- One-hot encode low cardinal categorical variables (e.g.: boundary_conditions can only take 3 values: NNF, NNN or FNF, it is transformed to a set of 3 one-hot columns)

hexagonal_eigenfrequency	young_modulus	poisson_ratio	density	unit_cell_height	base_length	side_length	structure_height	boundary_conditions_NNF	boundary_conditions_NNN
0.025196	0.136661	0.296296	1.000000	0.219336	0.000000	0.120795	0.233766	1.0	0.0
0.102807	0.136661	0.296296	1.000000	0.219336	0.000000	0.120795	0.233766	0.0	1.0
0.121274	0.136661	0.296296	1.000000	0.219336	0.000000	0.120795	0.233766	1.0	0.0
0.001805	0.000060	0.740741	0.096154	1.000000	1.000000	1.000000	1.000000	1.0	0.0
0.041387	0.083327	0.555556	0.178205	1.000000	1.000000	1.000000	1.000000	0.0	1.0
...
0.027609	0.001593	0.703704	0.173077	0.000000	0.285714	0.000000	0.000000	1.0	0.0
0.008704	0.046660	0.481481	0.993590	1.000000	1.000000	1.000000	1.000000	1.0	0.0
0.039443	0.001593	0.703704	0.173077	0.000000	0.285714	0.000000	0.000000	0.0	0.0
0.029058	0.046660	0.555556	0.330769	0.000000	0.285714	0.000000	0.000000	1.0	0.0
0.003659	0.001593	0.703704	0.173077	1.000000	1.000000	1.000000	1.000000	1.0	0.0

Figure 14: Processed dataset sample

6.3 Model selection

Now that the data is ready, we first build a set of ML models and evaluate them against our data. We will use 3 main metrics to evaluate our models:

- R^2 informs on the percentage of variance in the target variable explained by the explanatory features.
- Mean Absolute Error (MAE) tells us how far our predictions are from the groundtruth on average
- Root Mean Squared Error (RMSE) is similar to MAE but penalizes large errors (through a square operation)

Model	Test R^2	Test MAE (Hz)	Test RMSE (Hz)
Linear Regression	0.82	1152	1897
LASSO	0.82	1148	1897
Decision Tree	0.75	1067	2251
Random Forest	0.88	866	1653
XGBoost	0.89	831	1503

Table 1: Performance Metrics for Different Models

Based on this first round of model selection, the XGBoost model performs the best in our case with an R^2 of 0.89. We chose to select this model for the following modeling steps.

Gradient boosted algorithms

Gradient boosted algorithms are a kind of tree-based model. The GBT algorithm works by initially fitting a single decision tree to the data. It then evaluates the errors made by this tree and constructs a new tree that targets those errors, placing more emphasis on the misclassified instances. This iterative process continues, with each subsequent tree learning from the mistakes of the ensemble so far. If these models show great performance in a wide range of applications, they are often prone to overfitting (over-learning during the training phase), and we had to manipulate them carefully. We selected an XGBoost model, which is an efficient implementation of these algorithms.

7 Results interpretation

7.1 Model performance

The selected model scored an R^2 of 0.89, an MAE of 831 and an RMSE of 1503. We would like to highlight that, if this seems like reasonably good performance, it is highly dependant on the use case and desired precision. However, these models are very well scalable, and will very likely reach higher accuracy level as the training data grows.

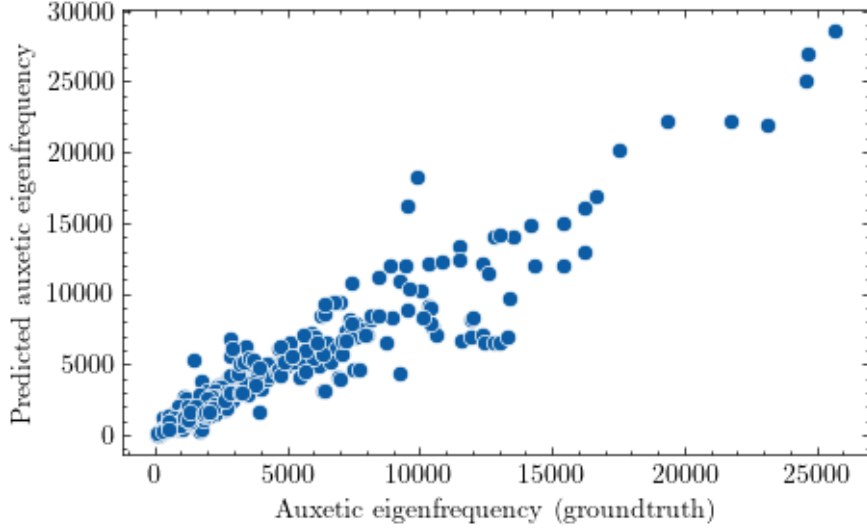


Figure 15: Scatterplot of model predictions against groundtruth

Moreover, the model reached a training R^2 of 0.999, indicating that it is overfitting the data. Again, increasing the dataset size is the main lever to reduce this phenomenon and maximize both accuracy and robustness.

7.2 Error analysis

In order to better understand our model's predictions and improve its performance, we performed an error analysis. Below is a visualization of the prediction errors' distribution (difference between predictions and actual values).

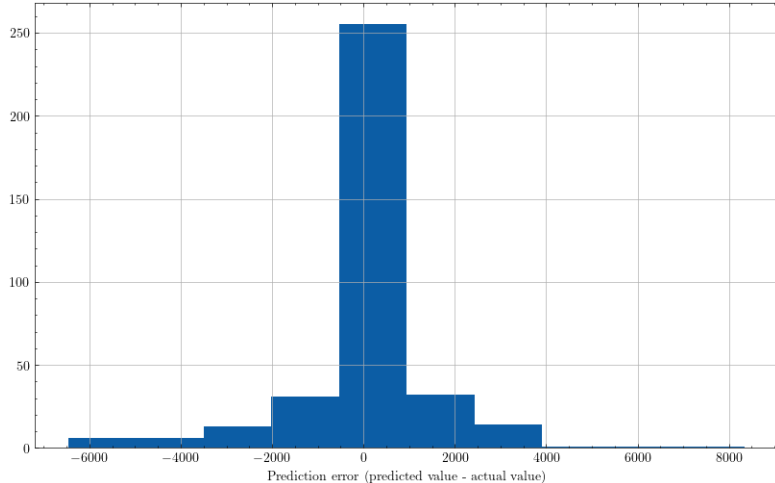


Figure 16: Distribution of prediction errors

The distribution is highly centered on 0, with over 75% of the errors laying in the [-400,400] interval. This shows good overall performance but highlights as well the presence of large errors (likely due to outliers visualized in the hexagonal-auxetic scatterplots). We further investigated the errors by plotting the histograms of errors for each frequency order (see Figure 23). Again, errors are particularly large for low order frequencies. To get a sense of this phenomenon, we plot the normalized mean absolute error for each frequency order: this metric represents the extent of the average absolute error compared to the average frequency for that order, i.e.: $\text{avg}(\text{error})/\text{avg}(\text{value})$, in the chart below.

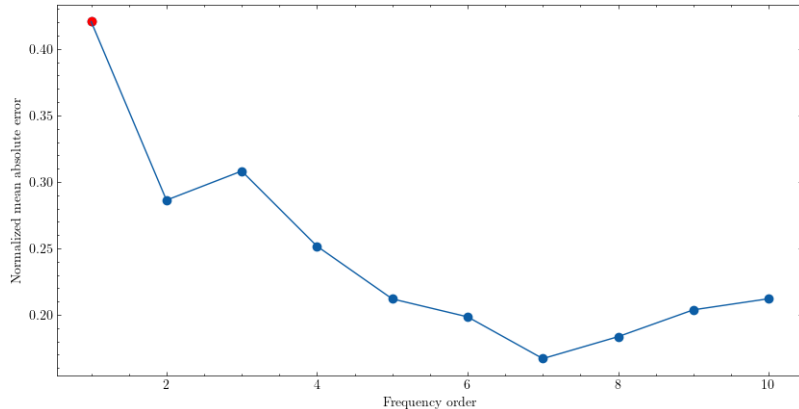


Figure 17: Normalized mean absolute error by frequency order

This chart captures again that low order frequencies (especially order 1 frequencies, represented by a red dot) are much harder to predict for our model. Errors represent typically 50% of the frequency value, which is considerable. This indicates inherent differences between frequency orders and their structure. Several approaches would help us reduce this effect and improve predictions for low frequencies:

- Increase training data: get more data examples, i.e. more materials and geometries, would certainly improve the performances on all observations.
- Train sub-models for all/groups of frequency orders. We could for example imagine a model trained on frequencies [1, 2, 3], another one on [4, 5, 6] etc.
- Add all hexagonal frequency orders to the training data (e.g.: use hexagonal frequencies 1 to 10 to predict auxetic frequency 1)

These last two techniques imply reducing the dataset size, and would therefore as well need to increase the original dataset to maintain a sufficient sample size for training our model.

7.3 Feature importance

Another crucial aspect of this work is understanding what factors influence the auxetic structures' behaviors and in what way. Here, we propose to use our model as a proxy to understand feature importances. The assumptions being that, if a feature is important for the ML model to generate the predictions, it deserves further study of its relation with the auxetics' eigenfrequencies. We use the XGBoost model's feature importance metric to evaluate our variables. The chart below shows feature importances for all 9 features used to generate the predictions.

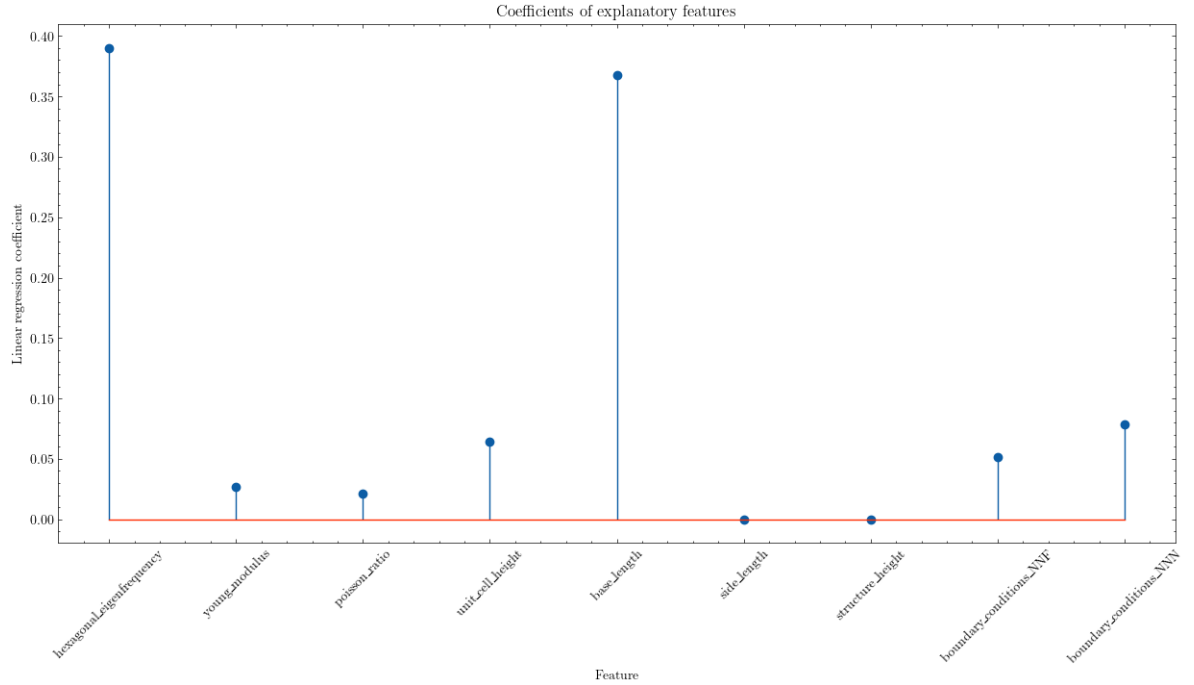


Figure 18: XGBoost model features importances

The results obtained are aligned with our initial exploratory analysis. Indeed, we highlighted in section 6.1 the high correlation between hexagonal and auxetic frequencies. It is no wonder that it is the top 1 important feature in our model. Following, we find geometry variables (especially base length), then others at a much lower importance level.

As the hexagonal frequency captures most of the importance when computing the predictions, we propose to run a version of the model without this feature, to investigate into the new importances of the other features. We expect this reduced model to be much less performant and we only view it as a tool to study the data variables.

Reduced model

The reduced model we train is a linear regression with all previous features except hexagonal_eigenfrequency. This will help evaluate both the intensity of the feature importance but also the direction of it (as linear regression coefficients can take negative values). The regression equation is the following:

```
auxetic_eigenfrequency ~ young_modulus + poisson_ratio + unit_cell_height + base_length
+ side_length + structure_height + boundary_conditions_NNF + boundary_conditions_NNN
```

The model explains 40% of the variance (note this would be higher if we built an XGBoost reduced model). The following chart shows the output features coefficients.

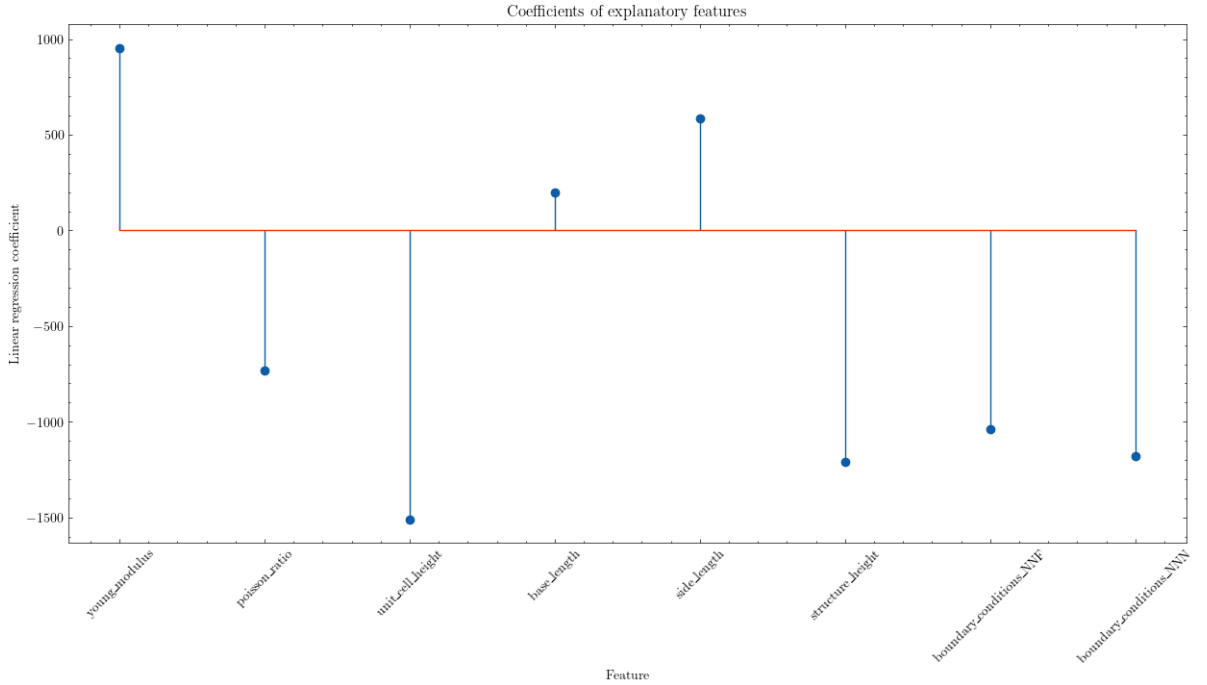


Figure 19: XGBoost model features importances (excluding hexagonal eigenfrequency)

The base_length feature has a much lower importance in this model. This could be explained by high correlations among the explanatory features. We especially observe that most geometric features have a negative correlation with the target variable. Finally, it's interesting to note that, the lower the poisson ratio, the higher is the auxetic natural frequency.

8 Applications and limits

One compelling example of the importance of considering a structure's natural frequency is the Tacoma Narrows Bridge. Located in Washington State, it is renowned for its catastrophic failure on November 7, 1940. This suspension bridge's collapse serves as a poignant reminder of the significance of understanding and considering the natural frequency of structures. Due to inadequate design considerations, the bridge's natural frequency coincided with the frequency of the wind gusts, resulting in destructive resonant vibrations. The repetitive excitation from the wind gradually amplified the amplitude of the oscillations, eventually overwhelming the bridge's structural integrity and leading to its tragic demise. [12] This pivotal event highlights the crucial role of accurately determining and accounting for the natural frequency of a structure in order to ensure its stability and avoid catastrophic failures. As catastrophic as it was, the Tacoma Bridge disaster could have been prevented through the implementation of modern natural frequency analysis methods, such as the ones presented in this study. They would have allowed engineers to identify and address the critical resonance issues that led to its catastrophic failure. It is an excellent example of the kind of applications where an ML model based off of natural frequency analysis would have proven very useful. The teams involved in the building of such a structure could have received invaluable information on the structure's integrity and the risks it poses. Most importantly, they would not have needed expert knowledge into FEA, or 3D modelling to extract that information and potentially prevent such a disaster.

While ML models have shown promise in predicting the behavior of auxetic structures and offer potential for various applications, it is important to acknowledge certain limitations. One limitation lies in the reliance on data quality and representativeness. ML models heavily depend on the availability of high-quality and diverse training data, which may not always be readily accessible or comprehensive. Additionally, the generalizability of ML models can be affected by the specific

characteristics of the training data, potentially leading to limited applicability to different materials or geometries not adequately represented in the dataset.

Furthermore, the application of ML models to new materials or scenarios requires caution and validation. ML models developed for a specific set of materials and geometries may not readily generalize to entirely different systems without proper validation and adjustment. It is crucial to conduct rigorous testing and validation to assess the model's performance and reliability in novel applications.

Limits

One significant limitation in this study is the constraint imposed by computational power, which directly affects the size of the generated dataset and subsequently impacts the accuracy of the ML model. Moreover, having access to a large data set could have allowed us to look at certain Deep Learning models to conduct our study. The use of these models, coupled with an expanded dataset, could have potentially yielded more accurate and nuanced predictions.

Another limitation to consider is the sole access to tabular data, neglecting the potential benefits of incorporating other data types, such as images. Images could have provided valuable visual information about the structures and materials, allowing the model to capture intricate details and patterns that may be missed with tabular data alone. Including image data in the analysis could have enhanced the predictive power and expanded the scope of the study.

In future research, overcoming computational limitations and exploring data types beyond tabular data, such as images, could lead to more comprehensive and accurate predictions of auxetic structure behavior. Expanding the dataset size and incorporating diverse data types would facilitate a deeper understanding of the relationships between materials, geometries, and natural frequencies, enabling more robust and effective ML modeling in this field.

9 Discussion

The findings of this study provide compelling evidence regarding the feasibility of utilizing ML models for applications beyond the present scope. The success of employing ML models to predict the behaviour of auxetic structures highlights their potential in diverse fields where similar predictive analyses are required. By demonstrating the effectiveness of ML models in this context, it becomes evident that their scalability and integrability make them an ideal platform for future studies in various disciplines.

The scalability and integrability of ML models are key factors that contribute to the expansion of this research. In fact, the scalability of ML models would allow for the analysis of larger and more complex systems, facilitating future investigation into the behaviour of complex structures in diverse scenarios. Additionally, the integrability of ML models would allow for easy incorporation into existing engineering tools and workflows. This integration aspect opens up numerous possibilities for expanding and refining the current study in future research endeavours.

Furthermore, if a similar modelling approach can be applied to study MEE (magneto-electro-elastic) materials, it would offer an innovative way to investigate their coupled properties. By leveraging the combination of FEA analysis and ML modelling, it would be possible to predict the effects of auxeticity on the coupled properties of MEE materials. This would not only provide valuable insights into the behaviour of these materials but also potentially replace the need for traditional eigenfrequency-based testing, offering a more efficient and cost-effective approach.

Considering the relatively new nature of research in the field of auxetic structures and ML modelling, the adoption of such techniques has the potential to accelerate the growth of knowledge in this domain. The scalability and repeatability of ML models also allows for the generation of large data sets and renders replication of experiments much simpler for future studies looking to add onto existing research. Over time, this improves the reliability and accuracy of any findings

made. Researchers can exploit ML models and their predictive power to explore the intricacies of meta-materials and contribute to the expanding knowledge pool of this emerging field.

References

- [1] Ken E Evans. "Auxetic polymers: a new range of materials". In: *Endeavour, Volume 15, Issue 4*, (1991), pp. 170–174.
- [2] Harshe Girish Avellaneda Marco. "Magnetolectric Effect in Piezoelectric/Magnetostrictive Multilayer (2-2) Composites". In: *Journal of Intelligent Material Systems and Structures 5* (1994), pp. 501–513.
- [3] Auxetic. 1996. URL: <http://www.worldwidewords.org/turnsofphrase/tp-aux1.htm>.
- [4] E. PAN and P.R. HEYLIGER. "FREE VIBRATIONS OF SIMPLY SUPPORTED AND MULTILAYERED MAGNETO-ELECTRO-ELASTIC PLATES". In: *Journal of Sound and Vibration 252.3* (2002), pp. 429–442. ISSN: 0022-460X. DOI: <https://doi.org/10.1006/jsvi.2001.3693>. URL: <https://www.sciencedirect.com/science/article/pii/S0022460X01936934>.
- [5] K. H. J. Buschow and F. R. de Boer. "Magnetostrictive Materials". In: *Physics of Magnetism and Magnetic Materials*. Springer US, 2003, pp. 171–175.
- [6] Qianchu Liu. "Literature Review: Materials with Negative Poisson's Ratios and Potential Applications to Aerospace and Defence". In: *DSTO Defence Science and Technology Organisation* (2006).
- [7] Ionut Ghinea. *Using FEA to study a mechanical part*. 2007. URL: <https://www.designworldonline.com/usingfea-to-study-a-mechanical-part/>.
- [8] A. Arockiarajan Naresh Pakam. "An analytical model for predicting the effective properties of magneto-electro-elastic (MEE) composites". In: *Computational Materials Science 65* (2012), pp. 19–28.
- [9] H. PUGA V. H. CARNEIRO J. MEIRELES. "Auxetic Materials – A Review". In: *Materials Science-Poland, 31(4)* (2013), pp. 561–571.
- [10] West H. Yang L. Harrysson O. "Modeling of uniaxial compression in a 3D periodic re-entrant lattice structure". In: *J Mater Sci 48* (2013), pp. 1413–1422.
- [11] E. Pan J.Y. Chen P.R. Heyliger. "Free vibration of three-dimensional multilayered magneto-electro-elastic plates under combined clamped/free boundary conditions". In: *Journal of Sound and Vibration 333* (2014), pp. 4017–4029.
- [12] Gianni Arioli and Filippo Gazzola. "A new mathematical explanation of what triggered the catastrophic torsional mode of the Tacoma Narrows Bridge". In: *Applied Mathematical Modelling 39.2* (2015), pp. 901–912. ISSN: 0307-904X. DOI: <https://doi.org/10.1016/j.apm.2014.06.022>. URL: <https://www.sciencedirect.com/science/article/pii/S0307904X14003424>.
- [13] Harvey West Li Yang Ola Harrysson and Denis Cormier. "Mechanical properties of 3D re-entrant honeycomb auxetic structures realized via additive manufacturing". In: *International Journal of Solids and Structures, Volumes 69–70* (2015), pp. 475–490.
- [14] Olly Duncan et al. "Quasi-static characterisation and impact testing of auxetic foam for sports safety applications". In: *Smart Materials and Structures, Volume 25, Number 5* (2016).
- [15] Richard Liang Aniket Ingrole Ayou Hao. "Design and modeling of auxetic and hybrid honeycomb structures for in-plane property enhancement". In: *Materials Design, Volume 117* (2017), pp. 72–83.
- [16] Benefit From Finite Element Analysis (FEA) In Your Manufacturing. 2019. URL: <https://www.goudsmit.co.uk/the-benefits-of-finite-element-analysisfea-in-manufacturing/>.
- [17] Kusum Meena and Sarat Singamneni. "A new auxetic structure with significantly reduced stress concentration effects". In: *Materials Design 173* (2019), p. 107779. ISSN: 0264-1275. DOI: <https://doi.org/10.1016/j.matdes.2019.107779>. URL: <https://www.sciencedirect.com/science/article/pii/S0264127519302163>.

- [18] Dhiren K. Pradhan, Shalini Kumari, and Philip D. Rack. "Magnetolectric Composites: Applications, Coupling Mechanisms, and Future Directions". In: *Nanomaterials* 10.10 (2020).
- [19] Shammo Dutta et al. "Study of auxetic beams under bending: A finite element approach". In: *Materials Today: Proceedings* 46 (2021). International Mechanical Engineering Congress 2019, pp. 9782–9787. ISSN: 2214-7853. DOI: <https://doi.org/10.1016/j.matpr.2020.10.479>. URL: <https://www.sciencedirect.com/science/article/pii/S2214785320381001>.
- [20] MJ Khoshgoftar and H Abbaszadeh. "Experimental and finite element analysis of the effect of geometrical parameters on the mechanical behavior of auxetic cellular structure under static load". In: *The Journal of Strain Analysis for Engineering Design* 56.3 (2021), pp. 131–138. DOI: [10.1177/0309324720957573](https://doi.org/10.1177/0309324720957573).
- [21] Tairidis G.K. Koutsianitis P.I. and Stavroulakis G.E. "Shunted piezoelectric patches on auxetic microstructures for the enhancement of band gaps". In: *Arch Appl Mech* (2021), pp. 739–751.
- [22] M. Vinyas. "Computational Analysis of Smart Magneto-Electro-Elastic Materials and Structures: Review and Classification." In: *Arch Computat Methods Eng* 28 (2021), pp. 1205–1248.
- [23] *FEA LIMITATIONS IN MECHANICAL ENGINEERING*. 2022. URL: <https://nkuleon.com/FEA-LIMITATIONS/>.
- [24] Genqiang Chen Yanfang Meng and Maoyong Huang. "Piezoelectric Materials: Properties, Advancements, and Design Strategies for High-Temperature Applications". In: *Nanomaterials (Basel)* 12 (2022), p. 1171.
- [25] *6 Benefits of F.E.A. in Designing Structural Engineering Materials*. URL: <https://acicorporation.com/blog/2019/10/11/6-benefits-of-f-e-a-in-designing-structural-engineering-materials/>.

A Exploratory data analysis

Histograms of eigenfrequencies for hexagonal and auxetic structures

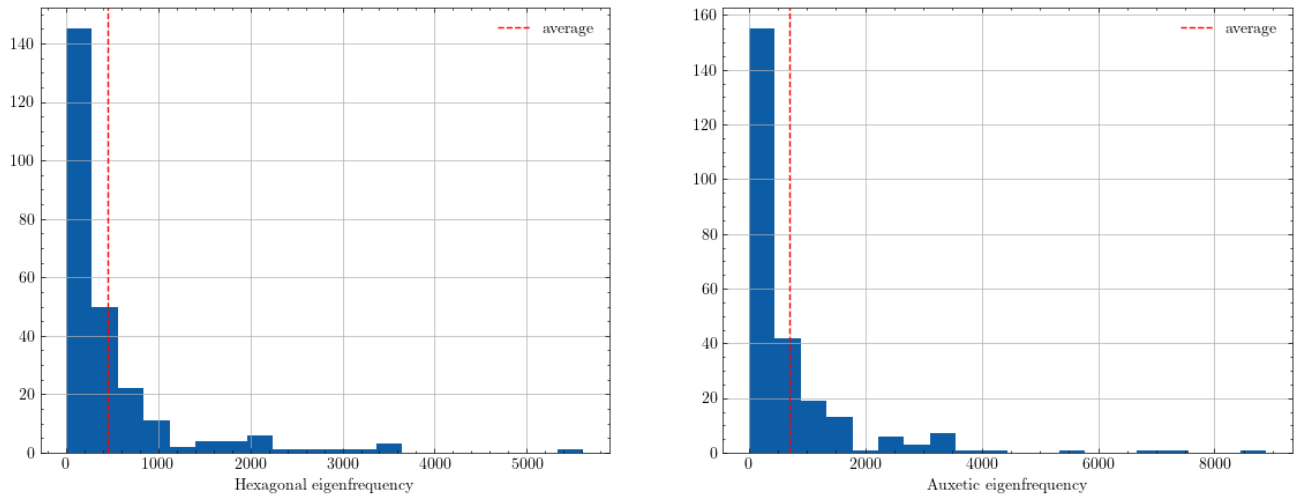


Figure 20: Histograms of hexagonal and auxetic natural frequencies

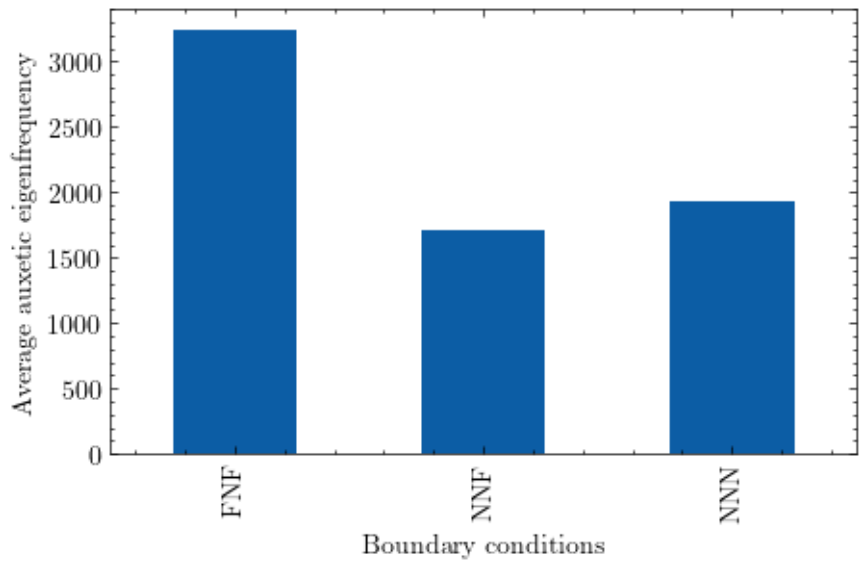


Figure 22: Average auxetic eigenfrequency for each boundary condition

OLS Regression Results						
Dep. Variable:	auxetic_eigenfrequency		R-squared:	0.836		
Model:	OLS	Adj. R-squared:	0.836			
Method:	Least Squares		F-statistic:	1.282e+04		
Date:	Thu, 11 May 2023		Prob (F-statistic):	0.00		
Time:	16:08:21		Log-Likelihood:	-21887.		
No. Observations:	2520		AIC:	4.378e+04		
Df Residuals:	2518		BIC:	4.379e+04		
Df Model:	1		Covariance Type:	nonrobust		
	coef	std err	t	P> t	[0.025	0.975]
Intercept	-44.8679	35.216	-1.274	0.203	-113.923	24.187
hexagonal_eigenfrequency	1.3946	0.012	113.233	0.000	1.370	1.419
Omnibus:	1359.705	Durbin-Watson:		0.250		
Prob(Omnibus):	0.000	Jarque-Bera (JB):		50919.846		
Skew:	1.906	Prob(JB):		0.00		
Kurtosis:	24.689	Cond. No.		3.53e+03		

Figure 21: Regression table for $f_n^a \sim f_n^h$

B Error Analysis

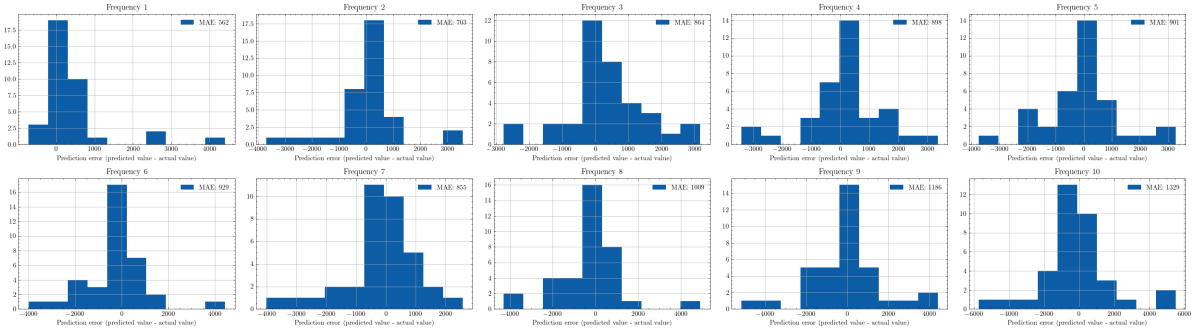


Figure 23: Prediction error histogram by frequency order

C MATLAB script for COMSOL simulations automation

```

function MATLAB_2()

models = {'A1', 'A2', 'A3', 'A4', 'H1', 'H2', 'H3', 'H4'};
boundary_conditions = {[26, 34], [26], []};
file_names = {'FNF', 'NNF', 'NNN'};

for i = 1:numel(models)
    model_name = models{i};

    for j = 1:numel(boundary_conditions)
        boundary_condition = boundary_conditions{j};
        file_name_suffix = strcat('_', model_name);
        file_name = strcat(file_names{j}, file_name_suffix);

        runModel(model_name, boundary_condition, file_name);
    end
end

function runModel(model_name, boundary_condition, file_name)
    model_file = fullfile('path/to/model/file');
    output_folder = 'path/to/output/folder';
    output_file = fullfile(output_folder, file_name);

    import com.comsol.model.*;
    import com.comsol.model.util.*;

    model = ModelUtil.create('Model');

    model.modelPath('path/to/model');

    model.component.create('comp1', true);

    model.component('comp1').geom.create('geom1', 3);

    model.component('comp1').mesh.create('mesh1');

```

```

model_file = fullfile('path/to/model/file');
model.component('comp1').geom('geom1').create('imp1', 'Import');
model.component('comp1').geom('geom1').feature('imp1').set('filename', model_file);
model.component('comp1').geom('geom1').feature('imp1').importData;
model.component('comp1').geom('geom1').run;

model.component('comp1').material.create('mat1', 'Common');
model.component('comp1').material('mat1').label('Nitinol');
model.component('comp1').material('mat1').propertyGroup('def').set('density', '1380');
model.component('comp1').material('mat1').propertyGroup('def').set('poissonsratio', '0.38');
model.component('comp1').material('mat1').propertyGroup('def').set('youngsmodulus', '4E+9');
model.component('comp1').material('mat1').set('groups', {});
model.component('comp1').material('mat1').set('family', 'plastic');

model.component('comp1').mesh('mesh1').automatic(false);
model.component('comp1').mesh('mesh1').feature('size').set('hauto', 4);

model.component('comp1').physics.create('solid', 'SolidMechanics', 'geom1');
model.component('comp1').physics('solid').create('fix1', 'Fixed', 2);
% Setting boundary conditions (26=bottom, 34=top)
if ~isempty(boundary_condition)
    model.component('comp1').physics('solid').feature('fix1').selection.set(boundary_condition)
end
model.study.create('std1');
model.study('std1').create('eig', 'Eigenfrequency');
model.study('std1').feature('eig').set('conrad', '1');
model.study('std1').feature('eig').set('solnum', 'auto');
model.study('std1').feature('eig').set('notsolnum', 'auto');
model.study('std1').feature('eig').activate('solid', true);
model.study('std1').feature('eig').set('neigsactive', true);
model.study('std1').feature('eig').set('neigs', 16);
model.study('std1').feature('eig').set('shiftactive', false);

model.sol.create('sol1');
model.sol('sol1').study('std1');

model.study('std1').feature('eig').set('notlistsolnum', 1);
model.study('std1').feature('eig').set('notsolnum', 'auto');
model.study('std1').feature('eig').set('listsolnum', 1);
model.study('std1').feature('eig').set('solnum', 'auto');

model.sol('sol1').create('st1', 'StudyStep');
model.sol('sol1').feature('st1').set('study', 'std1');
model.sol('sol1').feature('st1').set('studystep', 'eig');
model.sol('sol1').create('v1', 'Variables');
model.sol('sol1').feature('v1').set('control', 'eig');
model.sol('sol1').create('e1', 'Eigenvalue');
model.sol('sol1').feature('e1').set('eigvfunscale', 'maximum');
model.sol('sol1').feature('e1').set('eigvfunscaleparam', '1.09E-7');
model.sol('sol1').feature('e1').set('control', 'eig');
model.sol('sol1').feature('e1').feature('aDef').set('cachepattern', true);
model.sol('sol1').attach('std1');

model.result.create('pg1', 'PlotGroup3D');
model.result('pg1').set('data', 'dset1');

```

```

model.result('pg1').set('showlegends', false);
model.result('pg1').create('surf1', 'Surface');
model.result('pg1').feature('surf1').set('expr', {'solid.disp'});
model.result('pg1').label('Mode Shape (solid)');
model.result('pg1').feature('surf1').set('colortable', 'AuroraBorealis');
model.result('pg1').feature('surf1').create('def', 'Deform');
model.result('pg1').feature('surf1').feature('def').set('expr', {'u' 'v' 'w'});
model.result('pg1').feature('surf1').feature('def').set('descr', 'Displacement field');
model.result.evaluationGroup.create('std1EvgFrq', 'EvaluationGroup');
model.result.evaluationGroup('std1EvgFrq').set('data', 'dset1');
model.result.evaluationGroup('std1EvgFrq').label('Eigenfrequencies (Study 1)');
model.result.evaluationGroup('std1EvgFrq').create('gev1', 'EvalGlobal');
model.result.evaluationGroup('std1EvgFrq').feature('gev1').setIndex('expr', 'freq*2*pi', 0);
model.result.evaluationGroup('std1EvgFrq').feature('gev1').setIndex('unit', 'rad/s', 0);
model.result.evaluationGroup('std1EvgFrq').feature('gev1').setIndex('descr', 'Angular frequency');
model.result.evaluationGroup('std1EvgFrq').feature('gev1').setIndex('expr', 'imag(freq)/abs(freq)');
model.result.evaluationGroup('std1EvgFrq').feature('gev1').setIndex('unit', '1', 1);
model.result.evaluationGroup('std1EvgFrq').feature('gev1').setIndex('descr', 'Damping ratio');
model.result.evaluationGroup('std1EvgFrq').feature('gev1').setIndex('expr', 'abs(freq)/imag(freq)');
model.result.evaluationGroup('std1EvgFrq').feature('gev1').setIndex('unit', '1', 2);
model.result.evaluationGroup('std1EvgFrq').feature('gev1').setIndex('descr', 'Quality factor');

model.sol('sol1').runAll;

model.result('pg1').run;
model.result.evaluationGroup('std1EvgFrq').run;
model.result.table.create('tbl1', 'Table');
model.result.table.remove('tbl1');
model.result.evaluationGroup('std1EvgFrq').set('includeparameters', 'auto');
model.result.evaluationGroup('std1EvgFrq').feature('gev1').remove('unit', [0 1 2]);
model.result.evaluationGroup('std1EvgFrq').feature('gev1').remove('descr', [0 1 2]);
model.result.evaluationGroup('std1EvgFrq').feature('gev1').remove('expr', [0 1 2]);
model.result.evaluationGroup('std1EvgFrq').run;
model.result('pg1').run;
model.result.export.create('tbl1', 'Table');
model.result.export('tbl1').set('source', 'evaluationgroup');
file_path = fullfile('path/to/output/file', file_name);
model.result.export('tbl1').set('filename', output_file);
model.result.export('tbl1').run;

end

```